

The transverse resistivity in S/C multifilament wires studied through ac susceptibility measurements

P. Fabbriatore,¹ S. Farinon,¹ S. Incardone,¹ U. Gambardella,^{2,a)} A. Saggese,² and G. Volpini³

¹*Istituto Nazionale di Fisica Nucleare, Via Dodecaneso, 33, 16146 Genova, Italy*

²*CNR-INFN, Supermat Lab., Dipartimento di Fisica, Università di Salerno, 84081 Baronissi, Italy*

³*Istituto Nazionale di Fisica Nucleare, Via F.lli Cervi, 201, 20090 Milano, Italy*

(Received 24 July 2009; accepted 25 August 2009; published online 21 October 2009)

In this paper we discuss an experimental method based on the ac susceptibility for measuring the effective transverse resistivity in multifilament NbTi wires designed for low loss applications. Short samples of wire are involved in the measurements, with lengths comparable with the twist pitch. The measured values of the transverse resistivity are compared to expectations coming from a model based on a numerical approach. © 2009 American Institute of Physics. [doi:10.1063/1.3234378]

I. INTRODUCTION

Among the ac loss mechanisms in superconducting multifilament wires exposed to an ac transverse magnetic field, a relevant role is played by the coupling currents between filaments. Indeed, for some applications the reduction in the losses caused by the filament coupling is of crucial importance for keeping the overall losses at an acceptable level. The parameters affecting the coupling losses in a round wire are mainly two: the twist pitch of the wire and the transverse resistivity ρ_{et} . In general, the ac electromagnetic coupling losses in superconducting multifilament wires is a well known phenomenon, widely reported in the literature.¹⁻⁵ At the same time well established experimental methods for measuring the ac losses were developed, mainly based on magnetization measurements,⁶⁻⁹ involving even long samples of the wire. Nevertheless there are applications, such as the fast cycled superconducting dipoles for SIS300 synchrotron at FAIR,^{10,11} where the magnetic field is fast ramped at 1 T/s. These cases would require that the magnetization measurements were done at the same field ramp rate, which is usually higher, or much higher, than the ones allowed by the experimental setups, usually based on a superconducting magnet generating magnetic field larger than 3 T, with limitation with respect the field ramp rate.

Looking for a simple and reliable experimental method for obtaining information about the coupling ac losses, we have investigated the possible involvement of ac susceptibility measurement, which offers the advantage to have practically no limitations in the field rate. The use of ac susceptibility to investigate the coupling loss has also been proposed for HTS BSCCO/Ag tapes.^{12,13} On the other hand a couple of aspects need to be studied for understanding the real applicability of this method: (1) the samples are usually very short and comparable to the length of the wire twist pitch; (2) the ac field amplitude is low (0.1–10 mT) in comparison to standard magnetization measurements, even the one involving the minor cycles (1 mT or more). In this paper, after review-

ing the basic information coming from the ac susceptibility measurement in Sec. II, we present in Sec. III a method for obtaining the information related to the transverse resistivity ρ_{et} . In Sec. IV measurements done on different wires are reported and discussed, and the value of ρ_{et} is extracted. Finally, in Sec. V, a simple numerical method is presented for evaluating ρ_{et} and having an expectation to be compared with experimental values. Conclusions are drawn in Sec. VI.

II. AC SUSCEPTIBILITY

The ac susceptibility is a well known matter,¹⁴ but for this particular application we consider crucial to review the basic concepts in order to give a coherent formulation based uniquely on the measured quantities with a well defined physical meaning.

Let us consider a cylindrical sample of a superconducting multifilament wire (having radius R_s and length l_s) immersed in a oscillating magnetic field $B_{ext} = B_0 \cos \omega t$ transverse to the sample axis (directed along z). The wire is physically placed in a pick-up coil (having radius R_c and height h_c), which detects the magnetic flux variation. The superconducting shielding currents are generated in the sample, flowing in a thin layer close to the surface or through the bulk depending on the amplitude of the applied field and the critical current density J_c . These shielding currents generate a field opposed to the external field, so that, from a general point of view, the sample presents a diamagnetic magnetic moment $m(t)$. If the sample is small compared to the pick-up coil dimensions (R_s and $l_s \ll R_c$), the vector potential A at $r \gg R_s$ has, in cylindrical coordinates, only the angular component which can be expressed as¹⁵

$$A_{\vartheta}(z, r, t) = \mu_0 \frac{m(t)r}{4\pi(r^2 + z^2)^{3/2}}. \quad (1)$$

In Ref. 15 it has been shown that the magnetic flux Φ_c seen by the pick-up coil is

^{a)}Permanent address: INFN-Frascati National Laboratory, via E. Fermi, 40-00044 Frascati, Italy. Electronic mail: gamba@sa.infn.it

$$\Phi_c(t) = \mu_0 \frac{N_c}{h_c G_c} m(t), \quad \text{where } G_c = \sqrt{1 + \left(\frac{2R_c}{h_c}\right)^2} \quad (2)$$

being N_c the number of turns of the pick-up coil and G_c a geometrical factor.

Here we do not consider the flux contribution due to the external field because it can be easily canceled with a suitable arrangement of the experimental setup (e.g., using a second void pick-up coil). The voltage in the pick-up coil is simply the time derivative of the flux and consequently it is directly proportional to the time derivative of the magnetic moment.

Since the magnetic moment of the sample can be written as

$$m(t) = \sum_n m_n \cos(n\omega t + \varphi_n),$$

where φ_n are the phase shifts caused by the nonlinear response of the superconductor, the voltage in the pick-up coil V_{meas} is

$$V_{\text{meas}} = -\dot{\Phi}_c(t) = \mu_0 \frac{N_c}{h_c G_c} \sum_n m_n n \omega \sin(n\omega t + \varphi_n). \quad (3)$$

If this signal is sent to a lock-in amplifier filtering the first harmonic only, we have as output the in-phase voltage V_f and the out-of-phase voltage V_q ,

$$\begin{aligned} V_f &= \mu_0 \frac{N_c}{h_c G_c} m_1 \omega \sin \varphi_1, \\ V_q &= \mu_0 \frac{N_c}{h_c G_c} m_1 \omega \cos \varphi_1. \end{aligned} \quad (4)$$

It is possible to correlate the phase φ with physical quantities. With this aim, we need to write the magnetic field inside the sample in terms of the magnetic moment. The internal field B_{in} is given by $B_{\text{in}} = B_{\text{ext}} + \mu_0(1-D)M$, where B_{ext} is the external applied field, M is the sample magnetization (given by the magnetic moment m divided by the sample volume v_s), and D is the demagnetizing factor (0.5 in case of a cylinder in transverse field). We prefer using the external susceptibility $\chi_0 = 1/(1-D)$ rather than D . By using these definitions,

$$\begin{aligned} B_{\text{in}} &= B_0 \cos \omega t + \frac{\mu_0 m_1}{\chi_0 v_s} \cos(\omega t + \varphi_1) \\ &= \left(B_0 + \frac{\mu_0 m_1}{\chi_0 v_s} \cos \varphi_1 \right) \cos \omega t - \left(\frac{\mu_0 m_1}{\chi_0 v_s} \sin \varphi_1 \right) \sin \omega t. \end{aligned} \quad (5)$$

Indeed in Eq. (5) we should have had to consider the total magnetic moment $m(t)$, nevertheless, how we can see soon later, we will perform integration involving multiplication by the external field, so that only the first harmonics will survive.

We now compute the energy dissipated in the sample in a cycle,

$$\begin{aligned} W &= \oint_{\text{cycle}} M dB_{\text{ext}} = - \int_0^{2\pi} \frac{B_0 m_1}{v_s} (\cos \omega t \cos \varphi_1 \\ &\quad - \sin \omega t \sin \varphi_1) \sin \omega t d(\omega t) = \frac{B_0 m_1}{v_s} \pi \sin \varphi_1. \end{aligned} \quad (6)$$

Moreover, the average energy \mathcal{E} in the sample in a cycle,

$$\mathcal{E} = \frac{1}{T \mu_0} \int_0^T B_{\text{in}} B_{\text{ext}} dt = \frac{1}{2\pi} \left(\frac{B_0^2}{\mu_0} \pi + \frac{m_1 B_0}{\chi_0 v_s} \pi \cos \varphi_1 \right). \quad (7)$$

It is found that

$$\sin \varphi_1 = \frac{W v_s}{\pi m_1 B_0} = \frac{B_0 v_s}{2 \mu_0 \pi m_1} \frac{W}{\mathcal{E}_0} \quad \text{and} \quad \cos \varphi_1 = \frac{\frac{\mathcal{E}}{\mathcal{E}_0} - 1}{\frac{\mu_0 m_1}{\chi_0 B_0 v_s}}. \quad (8)$$

In these equations there is an apparent asymmetry: the expression with the $\cos \varphi_1$ contains χ_0 , but the expression with the $\sin \varphi_1$ does not. Actually there is no contradiction because χ_0 is included in W . When we have completed the analysis the final expression will not have this asymmetry.

Again we can consider only the first harmonic of the signal because, as we can see later, the signal is processed through a lock-in, which can select only this component of the field. Combining Eqs. (4) and (8) we have an explicit expressions for the signals in phase and out of phase,

$$\begin{aligned} V_f &= \frac{N_c}{h_c G_c} v_s B_0 \omega \left(\frac{1}{2\pi} \frac{W}{\mathcal{E}_0} \right), \\ V_q &= \frac{N_c}{h_c G_c} v_s B_0 \omega \left(\frac{\mathcal{E}}{\mathcal{E}_0} - 1 \right) \chi_0. \end{aligned} \quad (9)$$

These signals are related to the so-called ac susceptibility, which is a physical concept similar, but not coincident, to the magnetic susceptibility $\chi = dM/dH_{\text{ext}}$.

Since $dM/dH_{\text{ext}} = [1/(1-D)](dH_{\text{in}}/dH_{\text{ext}} - 1)$ (where the indexes in and ext are referred to the internal and external magnetic field H), we can write the susceptibility as $\chi = \chi_0(dH_{\text{in}}/dH_{\text{ext}} - 1)$.

In case of an harmonic external field $H_{\text{ext}} = H_0 e^{i\omega t}$, the internal field will be of the form $H_{\text{in}} = \sum_{n=1}^{\infty} (A_n - iB_n) e^{in\omega t}$. Considering the first harmonic only, the susceptibility can be written as

$$\begin{aligned} \chi &= (A_1 - iB_1) e^{i\omega t} \left(\frac{dH_{\text{in}}}{dt} \frac{dH_{\text{ext}}}{dt} - 1 \right) \\ &= \chi_0 \left[\frac{i\omega(A_1 - iB_1) e^{i\omega t}}{i\omega H_0 e^{i\omega t}} - 1 \right] \\ &= \chi_0 \left[\left(\frac{A_1}{H_0} - 1 \right) - i \frac{B_1}{H_0} \right]. \end{aligned}$$

The real and imaginary parts of the susceptibility are $\chi' = A_1/H_0 - 1$ and $\chi'' = B_1/H_0$, in the same way we did for the

signals V_f and V_q , it can be shown that the components of the susceptibility are related to the stored and dissipated energies,

$$\chi = \chi_0 \left[\left(\frac{\mathcal{E}}{\mathcal{E}_0} - 1 \right) - i \frac{W}{2\pi\mathcal{E}_0\chi_0} \right] = \chi_0[\chi' - i\chi'']. \quad (10)$$

Combining Eqs. (9) and (10), we have the final relations connecting the output signals and the components of ac susceptibility,

$$\begin{aligned} \chi' &= \frac{h_c G_c}{N_c v_s B_0 \omega \chi_0} V_q, \\ \chi'' &= \frac{h_c G_c}{N_c v_s B_0 \omega \chi_0} V_f. \end{aligned} \quad (11)$$

The measured signals V_q and V_f are directly proportional to the components of the ac susceptibility through a constant including the geometrical factors of the pick-up coil ($h_c G_c / N_c$, later denoted as g), the frequency, the peak ac field, the external susceptibility, and the volume v_s . This volume needs a remark as in the next pages we will refer to it as the *shielded volume* rather than the *sample volume*. The reason is that the systems under study are composite materials with superconducting filaments embedded in a normal conducting matrix. We will have situations where only the filaments are shielding the magnetic field (through permanent currents) and others where the whole wire is shielding the field through both filament permanent currents and currents generated by the filament coupling (crossing the matrix). The measured signals are directly proportional to the volumes involved in the shielding,

$$V_q = \frac{v_s B_0 \omega \chi_0}{g} \chi', \quad (12a)$$

$$V_f = \frac{v_s B_0 \omega \chi_0}{g} \chi''. \quad (12b)$$

III. AC SUSCEPTIBILITY AND COUPLING AC LOSSES

It is well known that the energy coupling loss per cycle and per unit volume of a multifilament wire exposed to a transverse harmonic field of peak value B_0 is¹⁶

$$W = \chi_0 \frac{B_0^2}{\mu_0} \pi \frac{\omega \tau}{1 + \omega^2 \tau^2}, \quad (13)$$

where τ is the characteristic time constant directly proportional to the square of the twist pitch p and inversely proportional to the transverse resistivity, $\tau = (\mu_0 / 2\rho_{el})(p/2\pi)^2$. Indeed, in the classical relation of the losses in a round wire, χ_0 of Eq. (13) is replaced by a factor of 2. Here we are using χ_0 not to lose generality. The coupling loss has a maximum at a characteristic frequency $f = 1/2\pi\tau$, allowing a precise measurement of τ . Since the component χ'' of the ac susceptibility is directly proportional to the ac loss, in principle we should be able to determine the characteristic time constant by analyzing the dependence of χ'' on the frequency. Due to

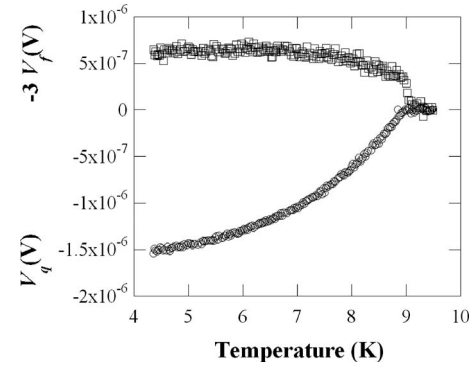


FIG. 1. Measured voltages V_q and V_f as a function of the temperature in a NbTi wire.

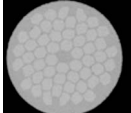
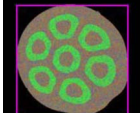
the direct connection between time constant and transverse resistivity, in the following pages we only focus on the time constant because it comes directly from measurements. The resulting transverse resistivity can be then easily deduced. In order to understand how these concepts can be applied, let us analyze the measurement shown in Fig. 1, where the signals V_f and V_q [hence the ac susceptibility components according to Eq. (12)] concerning a NbTi multifilament wire are plotted versus the temperature. In the following sections we will discuss with more details the geometrical characteristics of the samples under study, but here we are interested to the behavior of $\chi'(T)$ and $\chi''(T)$ for a generic multifilament wire.

It is important to know that this measurement is performed on a sample made of fine NbTi filaments ($\sim 2.6 \mu\text{m}$), placed transverse to an ac magnetic field $B_0 = 10 \text{ G}$ oscillating at 1.9 Hz, superimposed to a dc magnetic field $B_{dc} = 200 \text{ mT}$. The characteristic time constant for this sample is 5.1 ms, corresponding to a characteristic frequency of 31 Hz. As a consequence the frequency of 1.9 Hz can be considered to be a low frequency. The reason why we perform measurements at 0.2 T is related both to the occurrence of proximity coupling in these wires made of fine filaments (so the dc field depresses the proximity effect) and to the consideration that the application of a suitably small dc field simplifies the analysis, as the critical current density can be considered constant in the whole sample.

If the result in Fig. 1 is compared with classical ac susceptibility measurements, we find the following peculiarities.

- (1) In general $\chi'(T)$, i.e., the corresponding voltage V_q , is expected to decrease when lowering the temperature and to saturate to a value corresponding to the physical situation where the ac field in the NbTi filaments is completely shielded by the surface currents. In our case, the critical current density at 4.3 K for the NbTi is $J_c \approx 1.6 \times 10^{10} \text{ A/m}^2$ corresponding to a field penetration of 1 mT in a layer of thickness $\Delta x \sim B_0 / \mu_0 J_c = 0.05 \mu\text{m}$, i.e., much smaller than the filament dimension. In fact, the $\chi'(T)$ decrease is quite smooth and a saturation value is not yet clearly visible.
- (2) $\chi''(T)$, i.e., the corresponding voltage V_f , is expected to have a peak and then to decrease to zero as the temperature decreases. The peak value is related to the complete penetration of the ac field causing the largest possible

TABLE I. NbTi wire main features.

Wire	IGC 944-02-20	SL87969	Luvata_prototype
Cross section			
Diameter (mm)	0.651	0.811	0.825
Matrix	Cu/Mn	Cu/Mn	Cu/Mn
Twist Pitch (mm)	12.5	6.5	5
Matrix/SC	1.7	1.55	3.64
Filament diameter (μm)	2.63	2.5	2.5
Source	Provided by J. Kaugerts (GSI) micrograph by M. N. Wilson	Provided by J. K (GSI)	INFN/Luvata Fornaci di Barga (I)
Other information	Developed by H. Kanithi (IGC) for SSC		Developed in the frame of the DISCORAP project

dissipation, while the zero value is related to the quasi-complete shield of the magnetic flux. In fact, after a fast increase below T_c , $\chi''(T)$ never decreases to zero.

- (3) On the basis of the critical state model, the ratio between the maximum variations in χ' and χ'' is determined by the sample shape and field direction. One is expecting that $3\chi''_{\text{max}}/\chi'_{\text{max}} \approx 0.6-0.75$. In fact, the peak of χ'' is very small compared to the variation in χ' in the measured temperature range.

The observed behavior of $\chi'(T)$ and $\chi''(T)$ would suggest that we have to look at different basic mechanisms. In fact, the result of Fig. 1 can be interpreted considering that at low temperatures the ac susceptibility is dominated by the coupling currents (even at a frequency as low as 1.9 Hz), whereas the hysteretic effects are not contributing to losses because the low applied ac field (few gauss) is completely shielded by the filament surfaces. Under this view, the component χ'' at low temperatures (let us say in the 4–5 K temperature range), let us denote it as χ''_{cc} , would give a direct measurement of the ac losses due to the coupling currents. If this interpretation is correct, we would expect that at increasing frequencies, χ''_{cc} has a peak frequency at $1/2\pi\tau$ [as predicted by Eq. (13)]. At the same time the other component, χ'_{cc} , shall increase as the frequency increases because the coupling currents will shield larger and larger fractions of the wire. The limit of χ'_{cc} is at a frequency so high that the whole wire is shielded.

We tested this idea through ac susceptibility measurements on different multifilament wires. The experimental procedure was based on the measurements of $\chi'(T)$ and $\chi''(T)$ at fixed ac field (~ 10 G) performed at different frequencies.

IV. EXPERIMENTAL ANALYSES ON NbTi FINE FILAMENTS SAMPLE WIRES

The measurements were carried out on three different NbTi wires. The choice of the wires was determined by the

general frame, in which the authors are operating: i.e., the development of fast cycled superconducting dipoles.^{10,11} This application requires the involvement of low loss wires¹⁷ with small filaments (few microns), small twist pitches, and a relatively large transverse resistivity. One problem is just related to the transverse resistivity, which is enhanced through the dilution of Mn in the Cu matrix.¹⁸ A too high transverse resistivity could have negative effects on the wire thermal stability,¹⁷ so it is important to have a good knowledge of this parameter. In this framework we studied some wires produced in the past for applications requiring fast variations of the magnetic fields. Two samples were provided to us in small quantities, preventing us to perform measurements on very long samples (sample length much larger than its twist pitch). Furthermore a third wire, developed by Luvata, Fornaci di Barga, Italy under an INFN contract, was studied. In Table I the main parameters of the wires under study are reported.

For each sample two different lengths were used: (1) short samples with length approximately equal to the twist pitch and arranged in a straight configuration; (2) long samples, coil shaped (long two or three twist pitches) to fit the dimensions of the sample holder. The measurements were done in two different experimental setups, at INFN Genova and CNR-INFM at University of Salerno. Despite minor differences in electronic equipment between the setups, they share the same general layout shown in Fig. 2.

As explained in Sec. III, we focus the interest on the values of $V_{qcc}/(B_0f)$ and $V_{fcc}/(B_0f)$ versus the frequency f . The index cc has the same meaning as described in Sec. III. Figures 3(a)–3(c) report the measurements performed on the three wires. Each graph shows measurements on both short sample (≈ 1 twist pitch) and long sample (≈ 2 twist pitches). The measured values of V_{fcc} and V_{qcc} are divided by B_0f and normalized to the value of $V_{qcc}/(B_0f)$ measured at the lowest

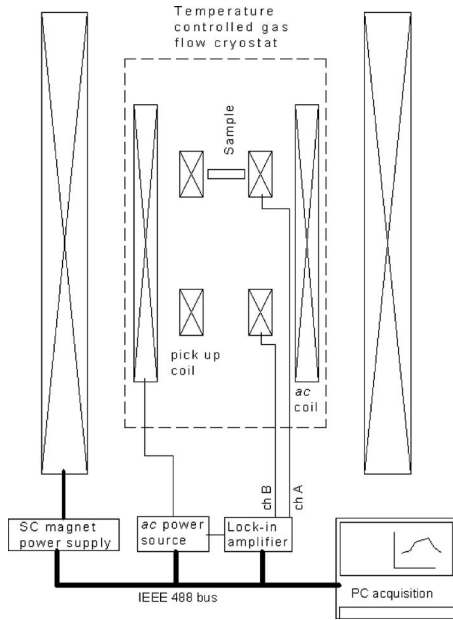


FIG. 2. Experimental setup for measuring the ac susceptibility at varying temperatures and applied dc magnetic field.

frequency, with the aim to have a clear normalization to a physical situation where only the filaments shield the magnetic field.

The experimental results concerning these three wires have many common aspects.

- (1) The quantity $V_{fcc}/(B_0f)$, which according to Eq. (8) is directly related to the energy dissipated in a cycle, shows a peak value when plotted as function of the frequency. This behavior is expected if Eq. (13) is applicable. The characteristic frequencies are 31 Hz for IGC sample, 87 Hz for SL sample, and 94 Hz for Luvata wire, corresponding to characteristic time constants $\tau=5.13$ ms, $\tau=1.83$ ms, and $\tau=1.69$ ms, respectively.
- (2) The shape of $V_{fcc}/(B_0f)$ is the same for both short samples and long samples and the peak values are placed at the same characteristic frequency. This is the most important result of this work as it can be seen as a strong mark of the coupling mechanism.
- (3) The quantity $V_{qcc}/(B_0f)$ is an increasing function of the frequency, as we can expect if the coupling currents are shielding more and more the wire. Commenting data in Fig. 1 we have already pointed out that we did not observe this case (dissipation is not zero; χ'_{cc} has not saturated at low temperatures). Nevertheless the extremely small slope of $V_{qcc}/(B_0f)$ as a function of f at low frequencies suggests that the magnetic shield is mainly due to the filaments. In Eq. (12a) we can see that V_{qcc} is directly proportional to the shield volume. So we should expect that when $f \rightarrow \infty$ the quantity $V_{qcc}/(B_0f)$ increases because the shielded volume is changing from the filaments to the whole wire volume. The limit value at high frequency cannot be higher than $1 + \alpha$ times the value at low frequency, being α the matrix to superconducting material (Matrix/SC) ratio. The maximum expected values for $V_{qcc}/(B_0f)$, from the Matrix/SC values listed in

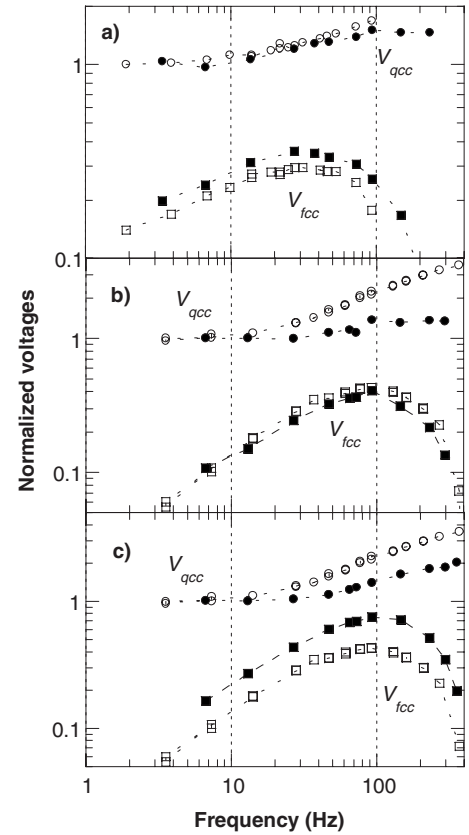


FIG. 3. Normalized ac susceptibility voltages V_{qcc} and V_{fcc} vs frequency at 4.5 K for IGC sample (a), SL87969 sample (b), and Luvata sample (c). The open and solid symbols refer to short and long samples, respectively. Normalization coefficients are the V_{qcc}/B_0f values measured at the lowest frequency. Measurements were performed in a dc magnetic field of 0.2 T.

- Table I, are therefore 2.7, 2.55, and 4.64, respectively, for samples IGC, SL, and Luvata. The experimental values of these factors at the maximum measured frequencies were 1.5–1.7 for the IGC wire, from 1.3 to 3.6 for the SL wire, and from 2.1 to 3.5 for Luvata wire. The discrepancies between experimental and expected values can be partly explained considering that also the external susceptibility χ_0 can be different for filaments and the wire. In fact, the filaments could have a $\chi_0 > 2$ due to their deformed shape.
- (4) If the main loss mechanism is due to the coupling currents and Eq. (13) is then applicable, we could expect that the peak value of χ'' , which using Eq. (10) is $\chi'' = \omega\tau/(1 + \omega^2\tau^2)$ would be 0.5. For $V_{fcc}/(B_0f)$ the peak shall be higher because we have to consider the normalization with respect to $V_{qcc}/(B_0f)$ at low frequency. In fact, we have to include both the amplification factor coming from the increasing with frequency of shielded volume and the external susceptibility variation from low to high frequency. This information is not predictable at the peak frequency (this frequency reflects an intermediate situation between low frequency and high frequency limits). As an attempt, we can directly take the measured $V_{qcc}/(B_0f)$ values at the frequency of the peak as the amplifying factors. For IGC wire the peak of $V_{fcc}/(B_0f)$ is ranging from 0.3 (short sample) to 0.35 (long sample); multiplying both by 1.3 [the measured

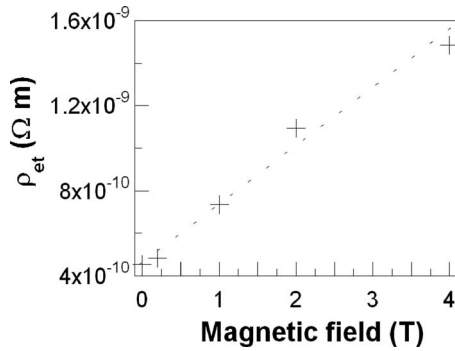


FIG. 4. ρ_{et} values at 4.5 K computed from measured characteristic frequencies on IGC wire as a function of the applied magnetic field.

$V_{qcc}/(B_0f)$ value at the peak frequency] we obtain a peak of χ'' ranging between 0.40 and 0.45. For SL wire the peaks of $V_{fcc}/(B_0f)$ are 0.41 (for both long and short samples). Multiplying by the factors of 1.3 and 2, we have a peak of χ'' ranging between 0.52 and 0.82. For Luvata wire the peaks of $V_{fcc}/(B_0f)$ are 0.41 (short sample) and 0.73 (long sample). Multiplying by the factors of 2.2 and 1.42, we have a peak of χ'' ranging between 0.90 and 1.07. These results are controversial: for IGC (both short and long samples) the peak values are 10%–20% lower than expected. For SL wire the long sample has the correct peak while the short sample has a peak 65% higher. For Luvata wire the peak is a factor of 2 higher than expected.

The resulting set of the experimental data leads to a general conclusion that only the frequency of the peak of $V_{fcc}/(B_0f)$ seems to have a clear physical meaning, related to the characteristic time constant. This is not surprising if considering that (1) at increasing frequency both shielded volumes and external susceptibility are changing in not a predictable way; (2) we are not able, due to the noise level, to perform measurements at a frequency less than 1 Hz in order to detect the shielding in the filaments without coupling currents. Thus we do not have a clear reference for the normalizing factor $V_{qcc}/(B_0f)$ at vanishing frequencies $f \rightarrow 0$.

For one of the wire under consideration there is a confirmation of this result in the literature. Figures 14 and 15 in Ref. 17 report data on the same IGC conductor. The measured transverse resistivity at 0.2 T is 0.453 n Ω m (see also Refs. 19 and 20). The corresponding characteristic time constant is 5.49 ms, to be compared with our result of 5.13 ms. In addition we show in Fig. 4 the $\rho_{et}(H)$ values computed from the characteristic frequencies measured for the IGC wire under different applied frequencies measured for the IGC wire under different applied magnetic field values. Again a good agreement is found comparing our data in Fig. 4 to data of Fig. 3 in Ref. 20, where a similar curve is reported from different experiment on the same wire.

Finally, a consideration is needed regarding the effect of the eddy currents on these results. In fact, in a multifilament wire exposed to a transverse field we have in the matrix both the transverse currents due to filament coupling and the longitudinal eddy currents closing at the wire ends. A simple conclusion can be drawn looking at the time constants. For the coupling currents the time constant is given by τ_{cc}

$= (\mu_0/2\rho_{et})(p/2\pi)^2$, for the eddy currents the maximum time constant (if the wire were completely made of copper) is $\tau_{eddy} = (\mu_0/8\rho_{Cu})R^2$, where R is the wire radius. The ratio between the two time constants is $\tau_{eddy}/\tau_{cc} = (\rho_{et}/4\rho_{Cu}) \times (2\pi R/p)^2$. For the wires under consideration this ratio ranges from 1.3% of the IGC wire to 14% of Luvata wire. Considering that the cross section allowed to the eddy currents for flowing is much smaller, these fractions are even smaller, leading us to neglect this effect.

V. INTERPRETATIVE MODELS

In order to obtain further confirmation to our interpretation of the experimental results, indicating that the peak of the $V_{fcc}/(B_0f)$ occurs at the frequency corresponding to the characteristic time constant for the coupling current even if the sample is short (one twist pitch) and the ac field extremely small (few gauss), we developed a simple interpretative model based on the work performed by Duchateau *et al.*²¹ Our aim is to calculate the transverse resistivity for a real wire, taking into account the real wire layout rather than a crude approximation based on a simplified shell model.

If the frequency of the applied ac field is low compared to the characteristic frequency (where the ac losses get a maximum), we can assume that the internal field is practically coincident with the external field. In this case in the wire cross section the voltage applied to a filament placed at a position (x, y) is

$$V(x) = \frac{\dot{B}_{ext}}{2\pi} px. \quad (14)$$

Here the ac field has direction \hat{x} .

In principle if we are able to model the cross section of the wire, apply this condition to the filaments, and solve the static electric problem (governed by the Laplace equation), we can find the correct current distribution. Actually we cannot model thousands of filaments, but we can consider the large bundles of filament and apply the conditions directly to the bundles. This approximation is not bad in our case, where the filaments in the bundles are embedded in a high resistivity CuMn local matrix, so that the coupling currents are flowing mainly through the Cu parts of matrix surrounding the bundles. On this basis we have considered a model of the wire as shown in Fig. 5 (for IGC wire layout). The red zones are the filament clusters considered as a single material having an electrical resistivity (according to the model of Carr¹) of

$$\rho_{Fil.bundle} = \frac{1 - \lambda}{1 + \lambda} \rho_{CuMn}, \quad (15)$$

where λ is the local filling factor of superconductor, $\lambda = 0.75$, and ρ_{CuMn} is the resistivity of the copper manganese matrix surrounding the filaments of the bundle. To be noted that Eq. (15) is valid in the case of good electrical bonding between filaments and matrix. Considering that $\rho_{CuMn} = 2.1 \times 10^{-8} \Omega$ m, we have $\rho_{Fil.bundle} = 3 \times 10^{-9} \Omega$ m. The white zone in Fig. 5 is the copper matrix with resistivity (at $T = 4.2$ K and $B = 0.2$ T) $\rho_{Cu} = 1.7 \times 10^{-10} \Omega$ m. The condition in Eq. (14) is applied to the boundary of the filament

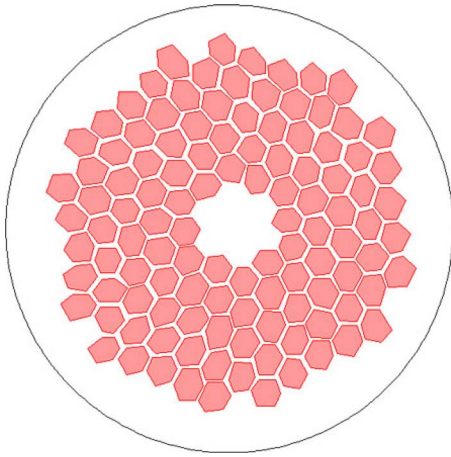


FIG. 5. (Color online) Geometrical model used for simulations.

bundles. The electric problem has been solved using the COMSOLTM finite elements code. With this approach we have $V(x=0)=0$. The obtained current distribution is shown in Fig. 6.

We can see that the currents are flowing both in the region external to the filaments and through the inner core. Once computed the current distribution we can now easily calculate the electrical dissipation integrating the local calculated electric field $\mathbf{E}(x,y)$ and the local current density $\mathbf{J}(x,y)$ over the cross section S , and dividing by the whole cross section,

$$W = \frac{1}{S} \int_S E(x,y)J(x,y) dx dy, \quad (16)$$

and finally obtain the time constant through

$$\tau = \frac{\mu_0 W}{2B_{\text{ext}}^2}. \quad (17)$$

The resulting time constant computed following this process is 5.38 ms, which compares very well with measured values (both ours and Wilson's reported result).

We have performed the same computation for SL and Luvata wires (see in Figs. 7 and 8 for the current distribu-

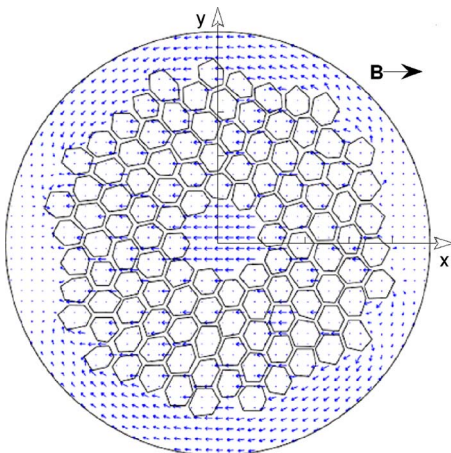


FIG. 6. (Color online) Coupling current distribution for IGC wire in its system coordinates. The arrows represent the total current density.

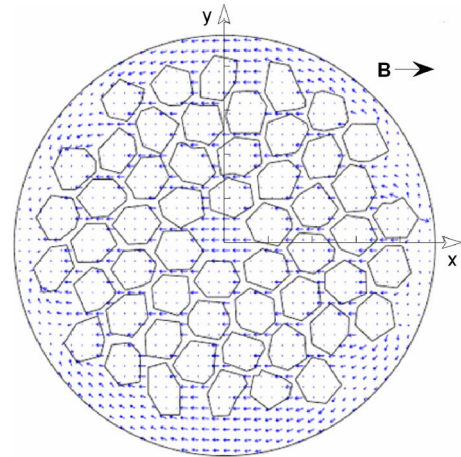


FIG. 7. (Color online) Coupling current distribution for SL87969 wire in its system coordinates. The arrows represent the total current density.

tions) obtaining a time constant of 1.61 and 1.57 ms, respectively (to be compared to the measured values of 1.81 and 1.69 ms).

VI. CONCLUSION

An experimental method based on ac susceptibility measurements has been developed for evaluating the time constant of the coupling currents in multifilament twisted wires. The method is based on the analysis of the components of the ac susceptibility versus the frequency of the ac magnetic field. Many aspects of these signals are controversial but one, the in-phase signal, has a well defined peak independent of the wire length (minimum one twist pitch). The frequency of the peak directly provides the time constant of the coupling mechanism (and hence the transverse resistivity). This has been verified by comparing the experimental results with a model involving a finite element analysis for solving the Laplace equation of a static electrical problem, which assumes that the voltage of any filaments is only given by the external flux variation. Practically the approach is the same used by Turk and Duchateau and recently reviewed by Wilson, only implementing a solution based on FEA.

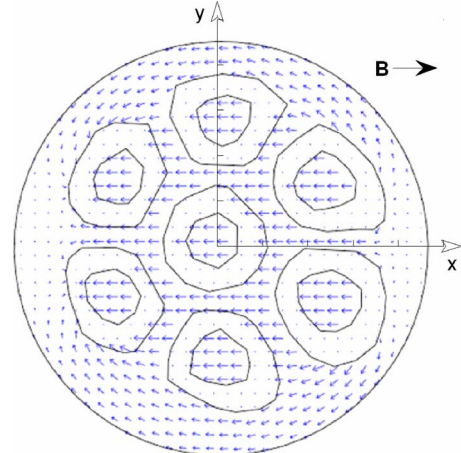


FIG. 8. (Color online) Coupling current distribution for Luvata wire in its system coordinates. The arrows represent the total current density.

ACKNOWLEDGMENTS

The authors are grateful to A. Ferrentino, University of Salerno, for his invaluable technical support. G. Moritz, GSI-Darmstadt, is acknowledged for the fruitful discussions and for his advices during the preparation of this paper.

¹W. J. Carr, *J. Appl. Phys.* **45**, 929 (1974).

²W. J. Carr, *J. Appl. Phys.* **45**, 935 (1974).

³G. Fournet and L. Boyer, Proceedings of the Sixth ICEC, 1976 (unpublished), p. 451.

⁴J. L. Duchateau and B. Turck, *Cryogenics* **14**, 545 (1974).

⁵M. N. Wilson, Proceedings of the International Conference on Superconductivity, Annapolis, 1972 (unpublished), p. 385.

⁶K. Kwasnitza and P. Bruzzone, *Cryogenics* **21**, 593 (1981).

⁷A. J. M. Roovers, W. Uijtewaal, H. H. J. ten Kate, B. ten Haken, and L. J. M. van de Klundert, *IEEE Trans. Magn.* **24**, 1174 (1988).

⁸T. Ogasawara, M. Itoh, Y. Kubota, K. Kanbara, Y. Takahashi, K. Yasohama, and K. Yasukochi, *IEEE Trans. Magn.* **17**, 967 (1981).

⁹M. M. Hlasnik, M. Majoros, and L. Jansak, in *Handbook of Applied Superconductivity*, edited by B. Seeber (IoP, Berkshire, 1998), p. 344.

¹⁰P. Fabbricatore, F. Alessandria, G. Bellomo, S. Farinon, U. Gambardella,

J. Kaugerts, R. Marabotto, R. Musenich, G. Moritz, M. Sorbi, and G. Volpini, *IEEE Trans. Appl. Supercond.* **18**, 232 (2008).

¹¹J. Kaugerts, G. Moritz, M. N. Wilson, A. Ghosh, A. den Ouden, I. Bogdanov, S. Kozub, P. Shcherbakov, L. Shirshov, L. Tkachenko, D. Richter, A. Verweij, G. Willering, P. Fabbricatore, and G. Volpini, *IEEE Trans. Appl. Supercond.* **17**, 1477 (2007).

¹²D. Zola, F. Gomory, M. Polichetti, F. Strycek, E. Seiler, I. Husek, P. Kovac, and S. Pace, *Supercond. Sci. Technol.* **17**, 501 (2004).

¹³D. Zola, F. Gomory, M. Polichetti, F. Strycek, J. Souc, P. Kovac, and S. Pace, *IEEE Trans. Appl. Supercond.* **15**, 2903 (2005).

¹⁴Fedor Gömöry, *Supercond. Sci. Technol.* **10**, 523 (1997).

¹⁵P. Fabbricatore, S. Farinon, F. Gomory, and S. Innocenti, *Supercond. Sci. Technol.* **13**, 1327 (2000).

¹⁶A. M. Campbell, *Cryogenics* **22**, 3 (1982).

¹⁷M. N. Wilson, *Cryogenics* **48**, 381 (2008).

¹⁸E. W. Collings, K. R. Marken, Jr., M. D. Sumption, E. Gregory, and T. S. Kreilick, *Adv. Cryog. Eng.* **36**, 231 (1990).

¹⁹H. C. Kanithi, P. Valaris, and B. A. Zeitlin, in *Supercollider III*, edited by J. Nonte (Plenum, New York, 1991) p. 689.

²⁰M. N. Wilson, GSI Report No. 25, 2006, available from g.moritz@gsi.de.

²¹J.-L. Duchateau, B. Turck, and D. Ciazynski, in *Handbook of Applied Superconductivity*, edited by B. Seeber (IoP, Berkshire, 1998) p. 205.